https://doi.org/10.5194/wcd-2019-6
Preprint. Discussion started: 13 September 2019

Weather and Climate Dynamics Discussions
Open Access
EGU

Extratropical cyclone induced sea surface temperature anomalies in the 2013/14 winter

Helen F. Dacre [1], Simon A. Josey [2], and Alan L. M. Grant [1]

[1]University of Reading
[2]National Oceanography Centre

Correspondence: H. F. Dacre (h.f.dacre@reading.ac.uk)

Abstract. The 2013/14 winter averaged sea surface temperature (SST) was anomalously cool in the mid-North Atlantic region. This season was also unusually stormy with extratropical cyclones passing over the mid-North Atlantic every 3 days. However, the processes by which cyclones contribute towards seasonal SST anomalies are not fully understood. In this paper a cyclone identification and tracking method is combined with ECMWF atmosphere and ocean reanalysis fields to calculate cyclone-relative net surface heat flux anomalies and resulting SST changes. Anomalously large negative heat fluxes are located behind the cyclones cold front resulting in anomalous cooling up to 0.2K/day when the cyclones are at maximum intensity. This extratropical cyclone induced 'cold wake' extends along the cyclones cold front but is small compared to climatological variability. To investigate the potential cumulative effect of the passage of multiple cyclone induced SST cooling in the same location we calculate Earth-relative net surface heat flux anomalies and resulting SST changes for the 2013/2014 winter period. Anomalously large winter averaged negative heat fluxes occur in a zonally orientated band extending across the North Atlantic between 40-60°N. The anomaly associated with cyclones is estimated using a cyclone masking technique which encompasses each cyclone centre and its trailing cold front. North Atlantic extratropical cyclones in the 2013/14 winter season account for 78% of the observed net surface heat flux in the mid- North Atlantic and net surface heat fluxes in the 2013/14 winter season account for 70% of the observed cooling in the mid-North Atlantic. Thus extratropical cyclones play a major role in determining the extreme 2013/2014 winter season SST cooling.

1 Introduction

The interaction of the ocean and atmosphere has long been recognised as an important element of oceanic cyclogenesis. In the tropics, sub-saturation of air above the sea surface in the vicinity of tropical cyclones results in strong surface heat fluxes which cool the upper ocean in the wake of tropical cyclones (Kleinschmidt, 1951; Fisher, 1958). In addition, strong winds enhance mixing in the upper-ocean, which can result in the transport of cool water to the surface. Similarly, in the mid-latitudes it was observed by Pettersen et al. (1962) that surface heat fluxes are largest in the advancing cold air mass behind an extratropical cyclone's cold front. Although fluxes are typically an order of magnitude smaller in extratropical cyclones than tropical cyclones, they still have the potential to influence the underlying ocean.

https://doi.org/10.5194/wcd-2019-6
Preprint. Discussion started: 13 September 2019

Weather and Climate Dynamics Discussions
Open Access
EGU

Alexander and Scott (1997) analyzed the association of ocean heat fluxes with propagating extratropical cyclones on synoptic timescales. They found positive flux anomalies (directed from the ocean to the atmosphere) in the western parts of the cyclones and the eastern parts of the cyclones were associated with negative turbulent flux anomalies. These results have been confirmed by many subsequent studies (Persson et al., 2005; Nelson et al., 2014; Schemm and Sprenger, 2015; Dacre et al., 2019) and suggest a close association between the cyclones and surface turbulent fluxes in the midlatitudes. However, a cyclone compositing study by Zolina and Gulev (2003) found that although composites of fluxes show locally very strong positive fluxes in the rear part of the cyclone, the total air-sea turbulent fluxes provided by cyclones were not significantly different from the averaged background fluxes in the North Atlantic.

The anomalous surface heat fluxes generated by cyclones can create SST anomalies known as the 'cold wake' effect. Case studies of winter cyclones in the North-West Atlantic have found SST cooling in the right-rear quadrant of cyclones of between 0.4 and 2 K (Ren et al., 2004; Nelson et al., 2014; Kobashi et al., 2019). This is largely due to enhanced turbulent fluxes behind the cold front, however Kobashi et al. (2019) also attribute part of the cooling to cloud shielding of incoming solar radiation, although this is possibly due to the more southerly latitude of the cyclone in their study. Cooling may also result from an episodic wind effect, known as resonance, whereby the rotation rate of the winds at a fixed point matches the rotation if the wind driven currents (Crawford and Large, 1996). The magnitude of the cooling has been shown to depend on the cyclone's intensity (Yao et al., 2008; Rudeva and Gulev, 2011) with stronger cyclones creating enhanced surface fluxes and hence increased cooling. In addition, there is some seasonality in the cooling magnitude, with largest cooling occurring in late summer and autumn when the surface mixed layer in the Northern Hemisphere is shallower (Ren et al., 2004; Kawai and Wada, 2011). Finally, the relationship between enhanced turbulent fluxes is regionally dependent. For example, Tanimoto et al. (2003) showed that in the central North Pacific, enhanced turbulent fluxes can generate local SST variations but in regions where ocean dynamics are important, such as the western Pacific, the SST anomalies formed in the early winter determine the mid- and late-winter turbulent heat flux anomalies rather than the passage of cyclones.

The effect of extratropical cyclone induced fluxes on longer timescale variability has been investigated in both the Atlantic and Pacific. Several studies have shown that wintertime fluxes in the Gulf Stream are characterized by episodic high flux events due to cold air outbreaks from North America associated with the passage of extratropical cyclones (Zolina and Gulev, 2003; Shaman et al., 2010; Parfitt et al., 2017; Ogawa and Spengler, 2019). Similar relationships have been found in the high-latitude South Pacific by Papritz et al. (2015). The influence of these enhanced fluxes is to restore the low-level atmospheric baroclinicity destroyed by the passage of the cyclones (Vannière et al., 2017) but the impact on the underlying SST's has not been quantified.

While the role of individual cyclones on local SST's have been studied, the cumulative effect of cyclone induced SST changes over individual seasons has not received much attention in the literature. Grist et al. (2016) found that during the winter of 2013/2014 enhanced sensible and latent heat fluxes occurred in the North Atlantic, with latent heat fluxes being largest in the east North Atlantic and sensible heat flux anomalies stronger in the west North Atlantic resulting in a reduction in ocean heat content of the subpolar gyre. The extent to which extratropical cyclones were responsible for these enhanced fluxes and associated cooling is not well understood.

https://doi.org/10.5194/wcd-2019-6
Preprint. Discussion started: 13 September 2019

In this paper we investigate both the SST cooling associated with individual cyclones and the SST cooling associated with the passage of multiple cyclones over the same location in the 2013/2014 season to determine how significant cyclones were in contributing to the observed cooling.

2 Data and Analysis Methods

2.1 ERA-Interim data

ERA-Interim is a global atmospheric reanalysis dataset (Dee et al., 2011). The data assimilation system used to produce ERA-Interim is based on Integrated Forecasting System (Cy31r2). The system includes a 4-dimensional variational analysis with a 12 hour analysis window. The spatial resolution of the data set is approximately 80 km (T255 spectral) on 60 vertical levels from the surface up to 0.1 hPa. 6 hourly ERA-Interim data has been used in this study to determine extratropical-cyclone related SST changes. We analyse several re-analysis fields from ERA-Interim which are described in this section.

The net surface thermal radiation (Q_{LW}) is the thermal radiation emitted by the atmosphere and clouds reaching the surface minus the amount emitted by the surface. Surface solar radiation (Q_{SW}) is the amount of solar radiation reaching the surface (both direct and diffuse) minus the amount reflected by the surface. Surface latent heat flux (Q_E) is the exchange of latent heat with the surface through turbulent diffusion and the surface sensible heat flux (Q_H) is the exchange of sensible heat with the surface. The magnitude of Q_E and Q_H depend on the windspeed and moisture and temperature differences between the surface and the lower atmosphere.

The net surface heat flux (Q_N) is given by the sum of Q_{SW}, Q_{LW}, Q_H and Q_E. The ECMWF convention for vertical fluxes is positive downwards. We also analyse ERA-Interim SST's which are the temperatures of sea water near the surface. ERA-Interim SST's are taken from different sources depending on the dates of the reanalyses: NCEP 2D-Var SST (Jan 1989 – Jun 2001); NOAA Optimum Interpolation SST v2 (Jul 2001 – Dec 2001); NCEP Real-Time Global SST (Jan 2002 – Jan 2009); Met Office Operational SST (Feb 2009 - 2015).

2.2 ECMWF Ocean Reanalysis System (ORAS5)

The ECMWF Ocean Reanalysis System 5 (ORAS5) is a global eddy-permitting ocean-sea ice reanalysis system. It provides an estimate of the historical ocean state from 1979 to present. The ocean model resolution in ORAS5 is 0.25 degree in the horizontal (approximately 25 km in the tropics, and increasing to 9 km in the Arctic) and 75 levels in the vertical. ORAS5 uses the Nucleaus for European Modelling of the Ocean (NEMO v3.4.1) ocean coupled to the Louvain-la-Neuve Sea Ice Model (LIM2) sea-ice model. It includes a prognostic thermodynamic-dynamic sea-ice model with assimilation of sea-ice concentration data (Zuo et al., 2017, 2019). The ocean mixed layer is the layer immediately below the ocean air-sea interface and is typically tens of meters deep in summer while values of several hundred meters may be reached in winter. In this paper the interannually and monthly varying mixed layer depth (MLD) from ORAS5 is used to calculate the SST tendencies (ΔSST) due to surface heat flux between 1989-2016. The ORAS5 MLD is the first depth at which the density difference, compared

https://doi.org/10.5194/wcd-2019-6
Preprint. Discussion started: 13 September 2019

Weather and Climate Dynamics Discussions
Open Access
EGU

to density at 10 m depth, reaches $0.01 \mathrm{kg/m}^3$. The Ocean Reanalysis MLD agrees well with the observationally based MLD estimates in the mid-Atlantic (Toyoda et al., 2017). However, in deep convective regions, such as the Labrador Sea, the density difference MLD definition can overestimate MLD (Courtois et al., 2017).

2.3 Cyclone identification

Following Dacre et al. (2012) we identify and track the position of the 200 most intense cyclones in 20 years of the ERA-Interim dataset (1989-2009) during wintertime only (DJF) using the tracking algorithm of Hodges (1995). Tracks are identified using 6-hourly 850 hPa relative vorticity, truncated to T42 resolution to emphasize the synoptic scales. The 850 hPa relative vorticity features are filtered to remove stationary or short-lived features that are not associated with extratropical cyclones. The intensity of the cyclones is measured by the maximum T42 vorticity. The 200 most intense DJF cyclone tracks with maximum intensity in the North Atlantic ($70° - 10°$ W, $30° - 90°$ N) are used in this study. These tracks are shown in figure 1(a). The cyclones generally propagate in a north-easterly direction, from the east coast of America towards Iceland. The position of the cyclones 24 hours before maximum intensity (*max -24*) are predominantly over the Gulf Stream (figure 1(b)). By maximum intensity (*max*) the majority of cyclones are located east of Newfoundland (figure 1(c)). During the decaying stage of the cyclones evolution (*max + 24*) the cyclones are more uniformly distributed across the North Atlantic (figure 1(d)).

2.4 Cyclone-relative composites

The fields, described in section 2.1, are extracted from ERA-Interim at each of the 6 hourly locations of the cyclone within a 30° radius surrounding the cyclone centre. Cyclone-relative composites are produced by averaging over all cyclones. Following Catto et al. (2010), before compositing the fields are rotated according to the direction of travel of each cyclone such that the direction of travel in the composite becomes the same for all cyclones. Since the cyclones have quite different propagation directions, performing the rotation ensures that mesoscale features such as warm and cold fronts are approximately aligned and are not smoothed out by the compositing. As this method assumes that the cyclones all intensify and decay at the same rate only the 200 most intense cyclones are included in the composite. Limiting the number of cyclones produces a more homogeneous group in terms of their evolution but will bias the mean fields to be typical of the most intense cyclones. Data are only included in the composite where grid points lie over ocean surface.

3 Results

3.1 North Atlantic heat flux and SST tendency climatologies

Figure 2 shows the average heat flux for the period DJF 1989-2015 over the North Atlantic. The net surface solar radiation is positive with a meridional gradient (figure 2(a)) and the net thermal radiation (figure 2(b)) is negative with a magnitude between -50 and -100 Wm^{-2}. The sensible heat flux (figure 2(c)) is generally positive over land and negative over the ocean with negative flux between -50 and -150 Wm^{-2} in the Gulf Stream and Davis Strait regions caused by the advection of cold

https://doi.org/10.5194/wcd-2019-6
Preprint. Discussion started: 13 September 2019

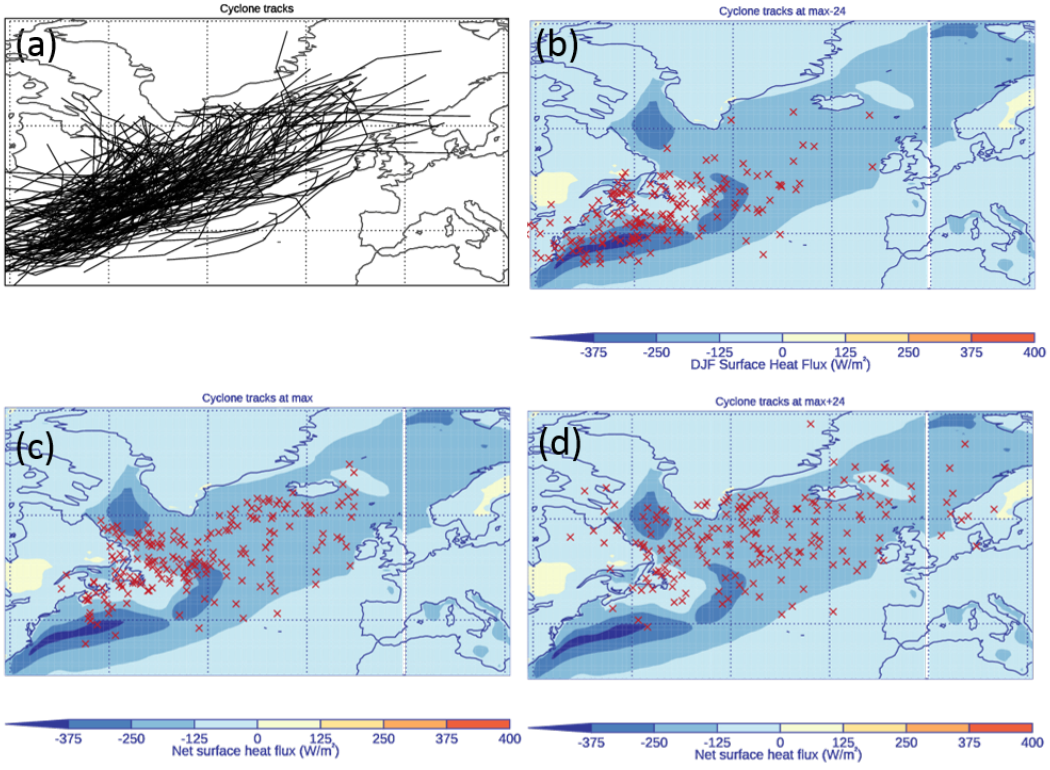

Figure 1. (a) Tracks of the 200 most intense DJF North-Atlantic storms between December 1989 and February 2009 (black). Position of the cyclones (b) 24 hours before maximum intensity (max-24), (c) at maximum intensity (max) and (d) 24 hours after maximum intensity (max+24) (red crosses). Overlaid on the DJF North Atlantic 1989-2015 net surface heat flux climatology (W/m^2).

air from the land over relatively warm oceans in DJF. The latent heat flux (figure 2(d)) is generally negative, with a band of enhanced negative flux extending in a north-eastwards direction from the east coast of the US towards Iceland with the values > 200 Wm^{-2} found in the west of the North Atlantic. The net heat flux, Q_N, (figure 2(e)), is negative over the majority of the domain. A combination of Q_H and Q_E results in maximum negative heat flux > 300 Wm^{-2} in the Gulf Stream region. The largest Q_N are co-located with the position of the North Atlantic storm track (figure 2(f)) which also exhibits a pronounced south-west to north-east tilt similar to the storm track in figure 1(a).

Figure 3(a) and (b) show the climatological SST and the average SST change over DJF (ΔSST_{TOT}) for the period 1989-2015. During DJF the North Atlantic cools by an average of 2K (figure 3(b)). The cooling is greatest where the SST gradient is largest in the Gulf Stream region (dotted box in figure 3(a)), with cooling of over 6 K over teh winter. Unlike the climatological Q_N shown in figure 2(e) the region of highest ΔSST_{TOT} does not extend over the North Atlantic towards Iceland but remains close to the east coast of the US.

https://doi.org/10.5194/wcd-2019-6
Preprint. Discussion started: 13 September 2019

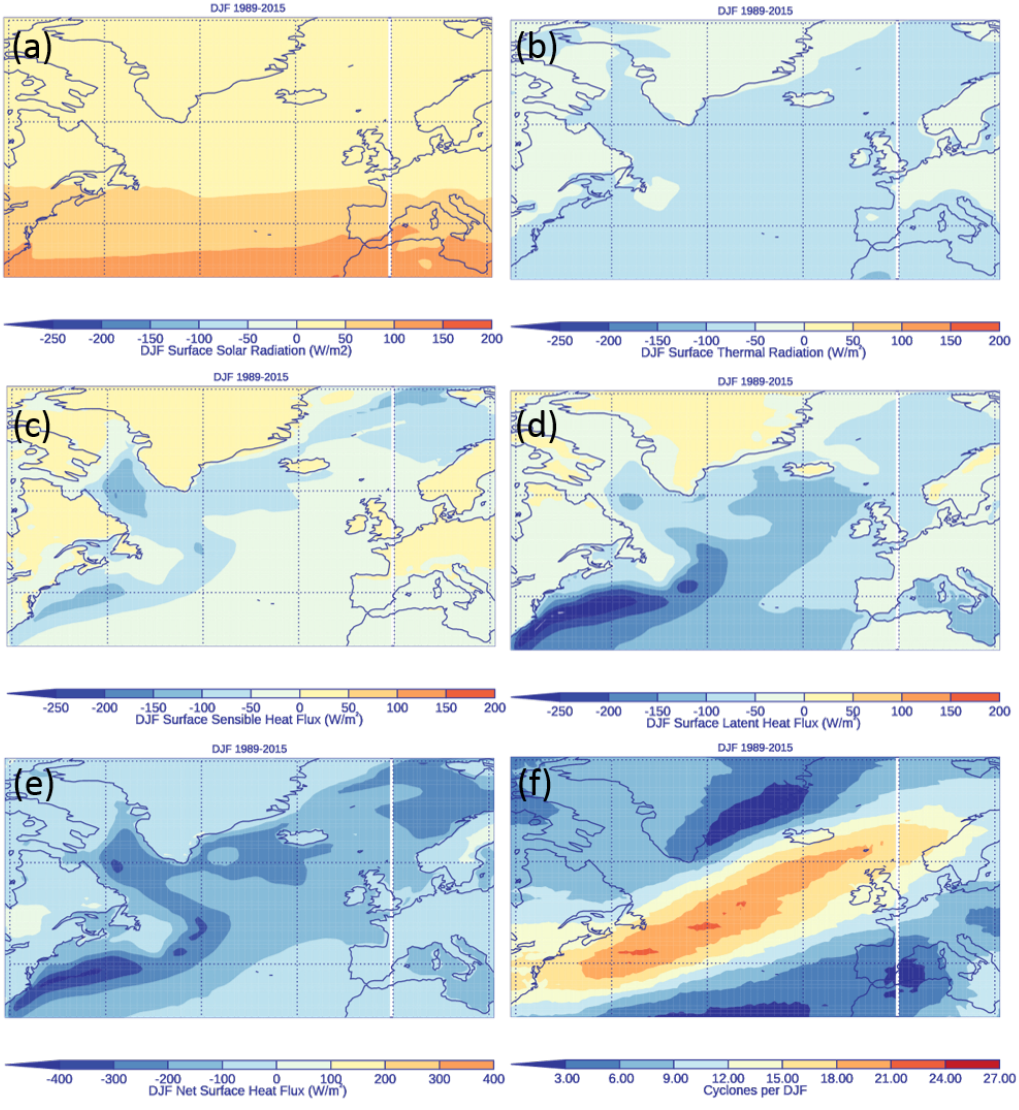

Figure 2. North Atlantic 1989-2015 heat flux climatologies (W/m^2). (a) Surface solar radiation, (b) surface thermal radiation, (c) surface sensible heat flux, (d) surface latent heat flux and (e) net surface heat flux. Note change in scale in figure (e). Positive flux is into the surface and negative flux is into the atmosphere. (f) 1989-2015 climatological number of cyclones per DJF season within 12° of grid point.

In order to calculate the SST tendency due to Q_N we must take into account the depth through which heating or cooling at the surface is mixed (h). Mixing in the ocean is assumed to occur between the surface and the mixed layer depth obtained from ORAS5. Assuming a well-mixed layer, the change in SST due to Q_N (ΔSST_{Q_N}) is given by;

$$\Delta\text{SST}_{Q_N} = \frac{\Delta t}{\rho c_p}\frac{Q_N}{h}, \tag{1}$$

https://doi.org/10.5194/wcd-2019-6
Preprint. Discussion started: 13 September 2019

Weather and Climate Dynamics Discussions
Open Access
EGU

where ρ is the density of sea water, 1000kgm^{-3}; c_p is the specific heat capacity of sea water, $4000\text{Jkg}^{-1}\text{K}^{-1}$ and Δt is the time (s) over which the ΔSST is calculated.

Figure 3(c) shows the climatological MLD. The MLD ranges from a few 10's of metres close to Newfoundland, to over 1000m in the Labrador and Norwegian seas where deep convection occurs. Taking the MLD into account restricts the largest ΔSST_{Q_N} to the western North Atlantic region (figure 3(d)). The difference between ΔSST_{TOT} and ΔSST_{Q_N} is shown in figure 3(e). Differences > 6K are found close to the coast where the western boundary currents transport warm waters north resulting in reduced cooling over the DJF period than would be expected due to Q_N alone.

3.2 Cyclone-relative heat flux composites

The north-south SST gradient in figure 2(e) is important for creating negative heat flux when cold dry air, from higher latitudes, is advected over relatively warm ocean surfaces. The largest heat flux occur when large differences in temperature or moisture between the surface and overlying atmosphere are co-located with enhanced wind speeds. Given the spatial distribution of SST's, atmospheric temperatures and moisture content, this is likely to occur when there are anomalously strong meridional winds such as are found ahead of and behind extratropical cyclones. Thus, whilst the maximum climatological SST gradient controls where locally high surface flux occur, the presence of extratropical cyclones are likely to control when the largest heat flux occur and their magnitude (Rudeva and Gulev, 2011). In addition, the similarities between the spatial pattern of climatological Q_N (figure 2(e)) and cyclone numbers per season (figure 2(f)) suggests that cyclones play a role in generating Q_N. In this section we investigate Q_N and SST tendencies in a cyclone-relative frame of reference using the methodology described in sections 2.3 and 2.4.

Figure 4 shows composite cyclone centred heat flux for the 200 most intense cyclones occurring between 1989-2009. The cyclones are at maximum intensity (maximum 850 hPa relative vorticity) when they are located at the centre of the domain and have been rotated so that they all travel from left to right. Q_{SW} (figure 4(a)) contribution to Q_N is positive and, like the Earth-relative perspective (figure 2(a)), there is a weak gradient. However, because the cyclones are typically travelling in a north-eastwards direction and they have been rotated, this gradient is also rotated. Q_{LW} (figure 4(b)) is negative everywhere and small, similar to the Earth-relative perspective. Q_{LW} is slightly enhanced in the region behind the cold front, potentially due to a reduction of cloud, which reduces the downwelling radiation. Q_H (figure 4(c)) shows a dipole structure at this stage in the cyclones evolution, with negative flux behind the cyclone centre and positive flux in the cyclones' warm sector. Q_E (figure 4(d)) is negative everywhere, a minimum in an extended region behind the cyclone and reduced ahead of the cyclone. Q_N (figure 4(e)) is therefore negative surrounding the cyclone centre with a minimum behind the cyclone. Negative flux > 200 W/m^2 occur within 1000 km of the cyclone centre but extend almost 2000 km in a westward direction due to a combination of Q_H and Q_E occurring behind the cold front.

In order to illustrate the processes leading to negative Q_H behind the cyclone cold front and positive Q_H in the warm sector it is necessary to examine the temperature characteristics of the different airmasses in these regions. Figure 5(a) and (b) show the composite 10 m air temperature and SST respectively overlaid with 925 hPa winds. The 10 m air temperature exhibits a wave like structure whilst the SST gradient is more linear. This results in a large negative near surface temperature difference

https://doi.org/10.5194/wcd-2019-6
Preprint. Discussion started: 13 September 2019

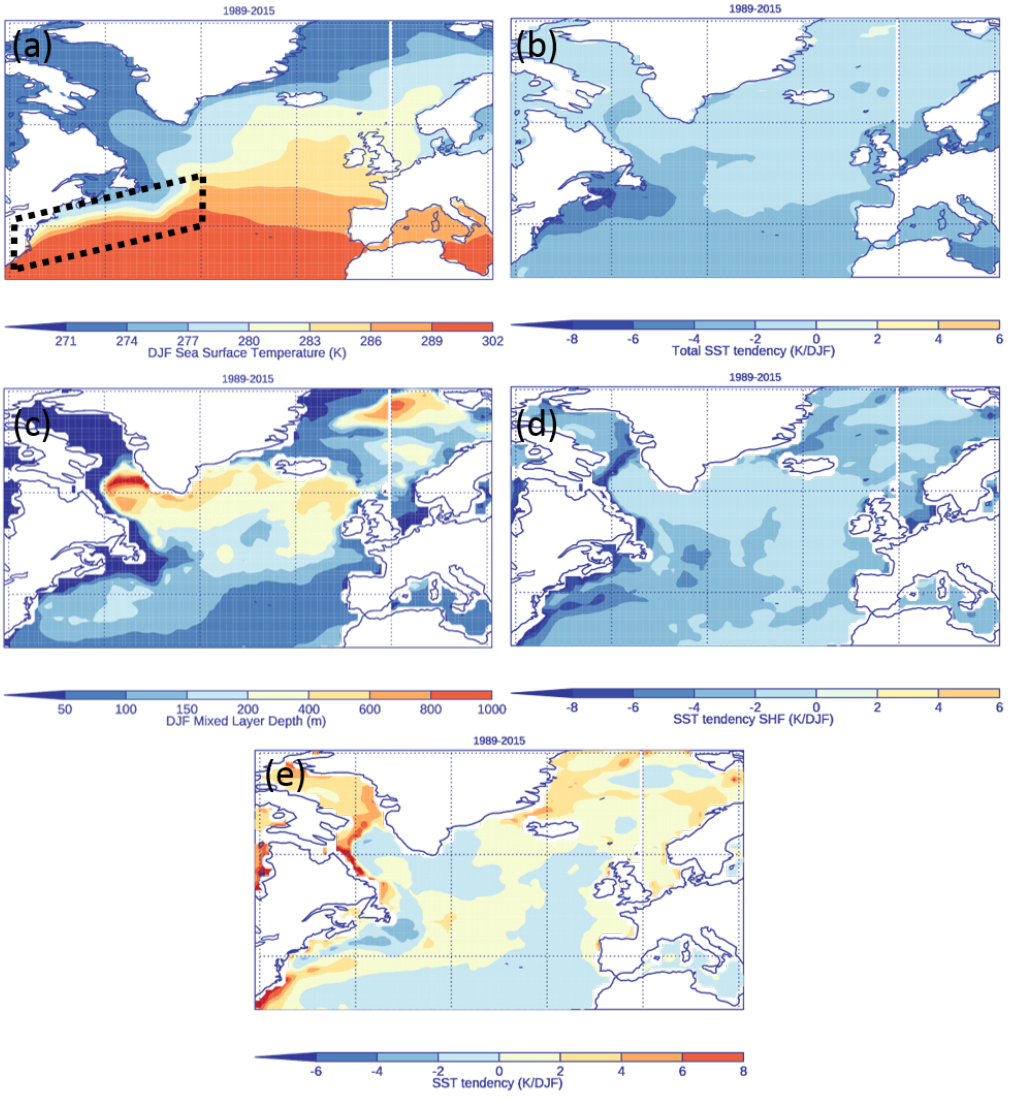

Figure 3. North Atlantic DJF 1989-2015 (a) sea surface temperature (SST, K), black dotted box outlines region of the Gulf Stream, (b) ΔSST_{TOT} (K/DJF), (c) mixed layer depth (m), (d) ΔSST_{Q_N} (K/DJF), (e) Difference between ΔSST_{TOT} and ΔSST_{Q_N}.

(SST $>$ 10 m temperature) behind the cold front. Cyclonic winds advect relatively cold air over a warm ocean surface behind the cyclone resulting in negative Q_H. Ahead of the cyclone cyclonic winds advect warm air over the ocean surface. 6 hours before maximum intensity the SST $<$ 10m air temperature ahead of the cyclone (not shown) but at maximum intensity the difference is close to zero (white contour in figure 5(b) shows -0.4 K). Since Q_H is a 6-hour average, this results in the positive Q_H observed in figure 4(c). Figure 5(d) and (e) show the 10 m specific humidity and the saturation specific humidity at the SST respectively. The 10 m specific humidity also has a pronounced wave structure with drier air behind the cold front and moister

https://doi.org/10.5194/wcd-2019-6
Preprint. Discussion started: 13 September 2019

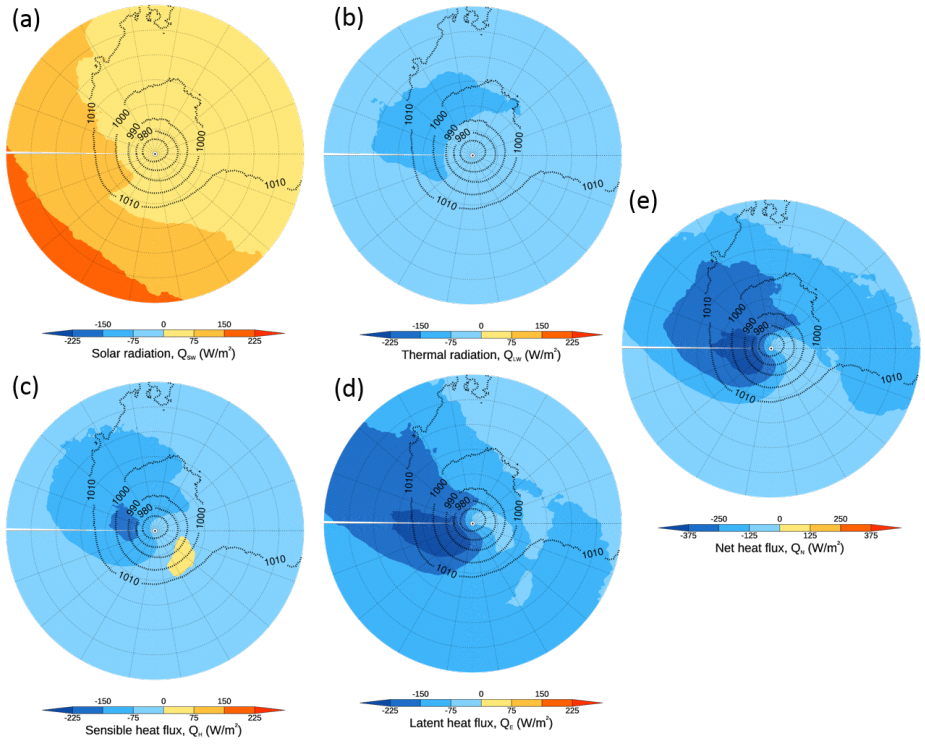

Figure 4. Composite cyclone centred heat fluxes (W/m^2) for cyclones at maximum intensity. (a) Surface solar radiation Q_{SW}, (b) surface thermal radiation Q_{LW}, (c) surface sensible heat flux Q_H, (d) surface latent heat flux Q_E and (e) net surface heat flux Q_N. Note the change in colour scale in figure (e). Positive fluxes are into the surface and negative fluxes are into the atmosphere. The radius of the circles is 3000 km and the cyclones are travelling from left to right.

air in the warm sector. Behind the cold front the saturation deficit is > 4 g/kg (figure 5(f)) causing evaporation of moisture from the surface and large negative Q_E observed in figure 4(d). Ahead of the cyclone the moisture deficit is < 1 g/kg significantly reducing the magnitude of Q_E.

Figures 6(a)-(c) show composite Q_N centred on cyclones at different stages in their evolution. As the cyclones start to intensify negative Q_N behind the cold front strengthens (figure 6(b)). During the mature stages of the cyclone evolution (figure 6(c)) Q_N begins to decrease and to wrap cyclonically around the cyclone centre. This is due to the fact that the cold front typically rotates cyclonically towards the warm front as the cyclone reaches maturity. These results are consistent with the findings of Rudeva and Gulev (2011) who found that turbulent heat flux increase with cyclone intensity.

Interestingly, throughout cyclone lifecycle there is a secondary minimum in Q_N occurring approximately 2000 km ahead of the cyclone location. This secondary minima does not change magnitude so is unlikely to be affected by the cyclones at the centre of the composite. It is possible that this second minima is due the presence of a downstream cyclone indicated by the composite mslp contours, which extend towards the upper-right quadrant of the domain.

https://doi.org/10.5194/wcd-2019-6
Preprint. Discussion started: 13 September 2019

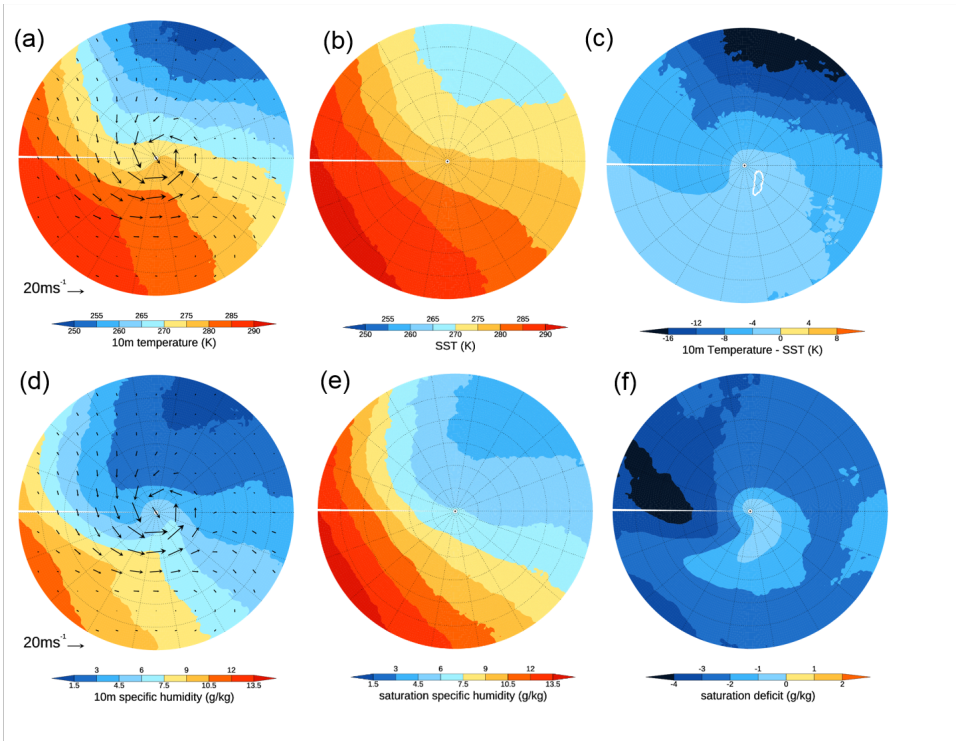

Figure 5. Cyclone centred fields at maximum intensity. (a) 10m Temperature (K), (b) SST (K), (c) 10m temperature - SST (white contour is -0.4 K) (K), (d) 10m specific humidity (g/kg), (e) saturation humidity of SST (g/kg), (f) 10m specific humidity - saturation humidity of SST (g/kg). (a) and (d) overlaid with 925hPa winds.

Since many of the 200 cyclones contributing to the composite Q_N (figure 4(e)) are generated over the Gulf-Stream region it is possible that large negative Q_N occurring behind of the cyclone centre could be an artifact of their preferential cyclogenesis over a region of climatologically large negative Q_N (figure 2(e)). To determine how Q_N compares to the background values we normalise Q_N anomalies by subtracting the climatological field at the position of each cyclone and divide by the standard deviation of the climatology at the same location. Figures 6(d)-(f) show normalised Q_N anomalies at different stages of the cyclone evolution. Negative anomalies indicate anomalously large heat flux into the atmosphere, with a value of -1 being 1 standard deviation larger than the climatological mean. Positive anomalies indicate anomalously small heat flux into the atmosphere, with a value of +1 being 1 standard deviation smaller than the climatological mean. At all stages of the cyclone evolution negative Q_N behind the cyclone centre is more than 0.5 standard deviations greater than the mean for strong cyclones and is more than 1 standard deviations greater than the mean at maximum intensity (figure 6(e)). Ahead of the cyclone Q_N is $0.4 - 0.8$ standard deviations greater than the mean at maximum intensity (figure 6(e)) due to warm air advection in the warm sector of the cyclone. Note that towards the edges of the domain many of the gridpoints are over land so have been excluded, therefore the sample size contributing to the composites is small resulting in noisy field.

https://doi.org/10.5194/wcd-2019-6
Preprint. Discussion started: 13 September 2019

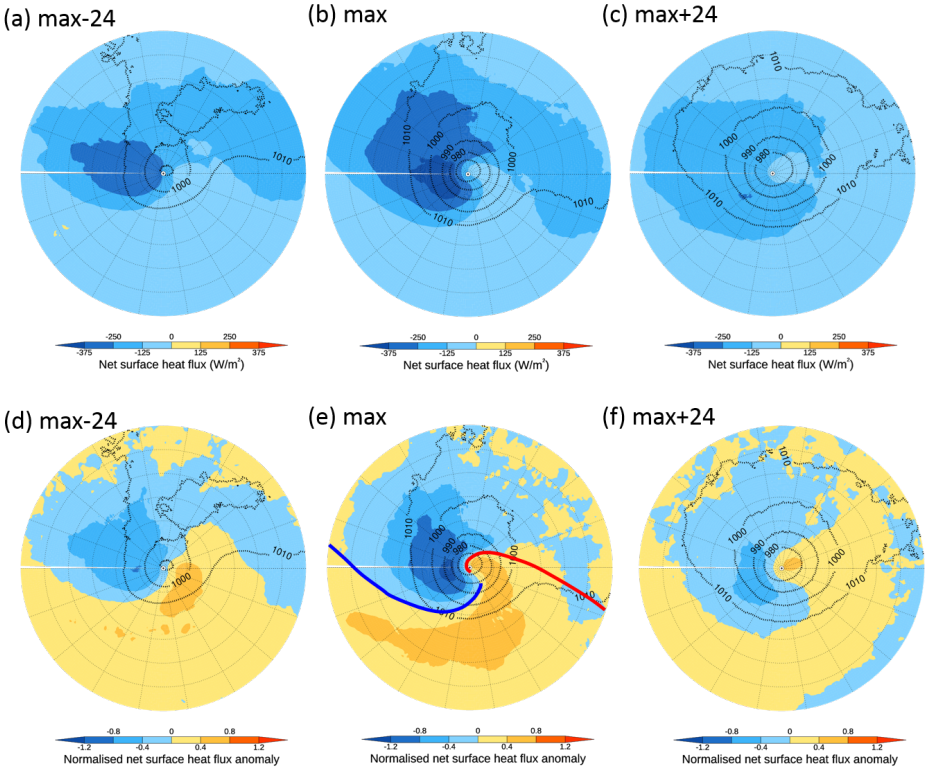

Figure 6. Evolution of cyclone centred (a)-(c) net surface heat flux Q_N (filled contours, W/m^2), (d)-(f) Normalised net heat flux anomaly (filled contours) and mslp (black contours, hPa). Cyclones reach the centre of the domain (a),(d) 24 hours before maximum intensity, (b),(e) at maximum intensity and (c),(f) 24 hours after maximum intensity. In (d)-(f) Negative normalised heat flux anomalies indicate anomalously large heat flux into the atmosphere and positive anomalies indicate anomalously small heat flux into the atmosphere compared to climatology. The blue and red lines in (e) represent the approximate positions of the cold and warm fronts at max intensity.

3.3 Cyclone-relative SST tendency

Using equation 1 the evolution of the cyclone-relative SST tendencies due to Q_N can be estimated. Figure 7 shows ΔSST_{Q_N} per day for cyclones at different stages in their evolution. The patterns of ΔSST_{Q_N} are similar to the patterns of Q_N (figure 6(a)-(c)) showing that surface flux is the dominant variable in the cooling and that variations in mixed layer depth are less important. As for Q_N, ΔSST_{Q_N} increases as the cyclones reach maximum intensity with maximum SST tendencies of 0.2K/day occurring in the cold sector behind the cold front. The normalised ΔSST_{Q_N} anomalies are calculated by subtracting the climatological ΔSST_{TOT} and dividing by the standard deviation of ΔSST_{TOT} (figures 7(d)-(f)). ΔSST_{Q_N} is larger than the climatological mean behind the cold front. However in this case the intense cyclones only reduce ΔSST by up to 0.25 times the standard deviation.

https://doi.org/10.5194/wcd-2019-6
Preprint. Discussion started: 13 September 2019

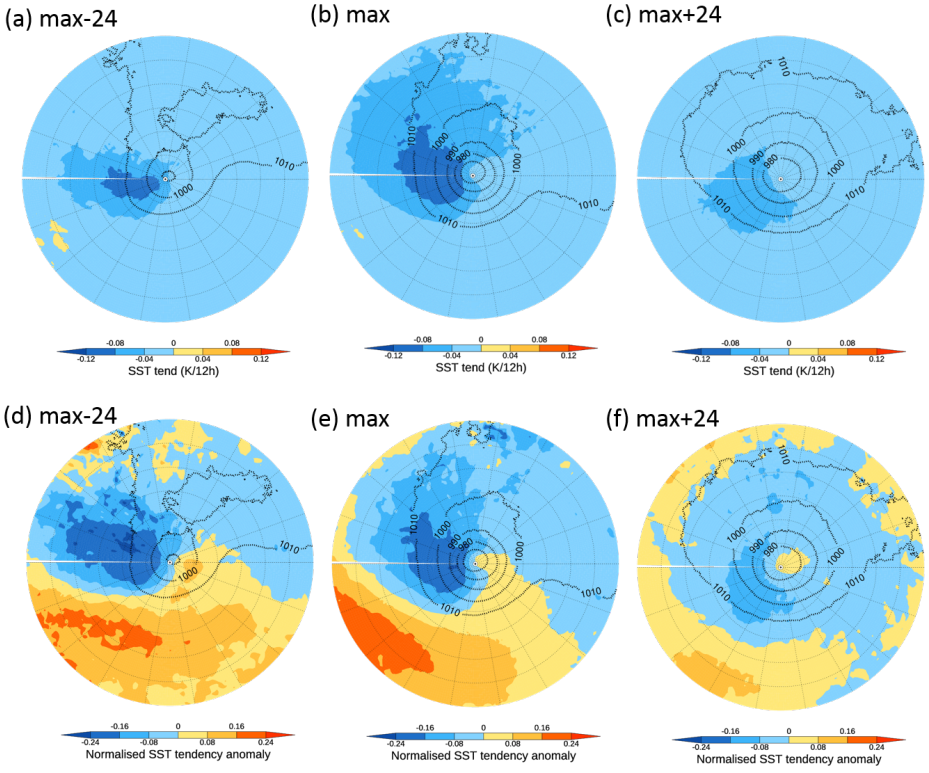

Figure 7. Evolution of cyclone centred (a)-(c) ΔSST_{Q_N} (filled contours, K/day), (d)-(f) Normalised ΔSST_{Q_N} anomaly (filled contours) and mslp (black contours, hPa). Cyclones reach the centre of the domain (a),(d) 24 hours before maximum intensity, (b),(e) at maximum intensity and (c),(f) 24 hours after maximum intensity. In (d)-(f) Negative normalised ΔSST_{Q_N} anomalies indicate anomalously large SST cooling due to Q_N and positive anomalies indicate anomalously small SST cooling compared to climatology.

4 2013/2014 heat flux anomalies

ΔSST_{Q_N} cooling associated with each individual extratropical cyclone is of the order $0.1-0.2$K/day (figures 7(a)-(c)) therefore if many cyclones track over the same location we might expect to see a signature of the storm track in the seasonal Q_N and SST anomaly patterns. Figure 8(a) shows the tracks of cyclones in the North Atlantic region. During the 2013/2014 winter the cyclones track in a south-west to north-east direction in a narrow band that extends from the east coast of the US towards the UK (figure 8(b)). This season was unusually stormy in the UK with cyclones passing over the UK every 3 days (Priestley et al., 2017). In comparison to the 1989-2015 average (figure 8(c)) the 2013/2014 the storm track was more active, with a higher number of cyclones and also more zonal than usual (figure 8(d)). More cyclones travelled towards western Europe than Iceland than usual.

It was shown in figure 6 that intensifying cyclones create negative Q_N behind the cold front, where cold dry air is advected over a warm ocean surface. Therefore we hypothesise that an anomalously strong and zonal storm track will result in an

https://doi.org/10.5194/wcd-2019-6
Preprint. Discussion started: 13 September 2019

220 anomalously strong and zonally orientated seasonal Q_N anomaly. The 2013/2014 DJF season Q_N is shown in figure 8(e) and the 2013/2014 Q_N anomaly shown in figure 8(f). The seasonal Q_N anomaly has a tripole pattern, with stronger negative Q_N in the mid-North Atlantic and weaker negative Q_N over the Gulf Stream and in the Norwegian and Greenland Seas. This is consistent with the shift in the storm track, with cyclones travelling zonally from the US towards western Europe.

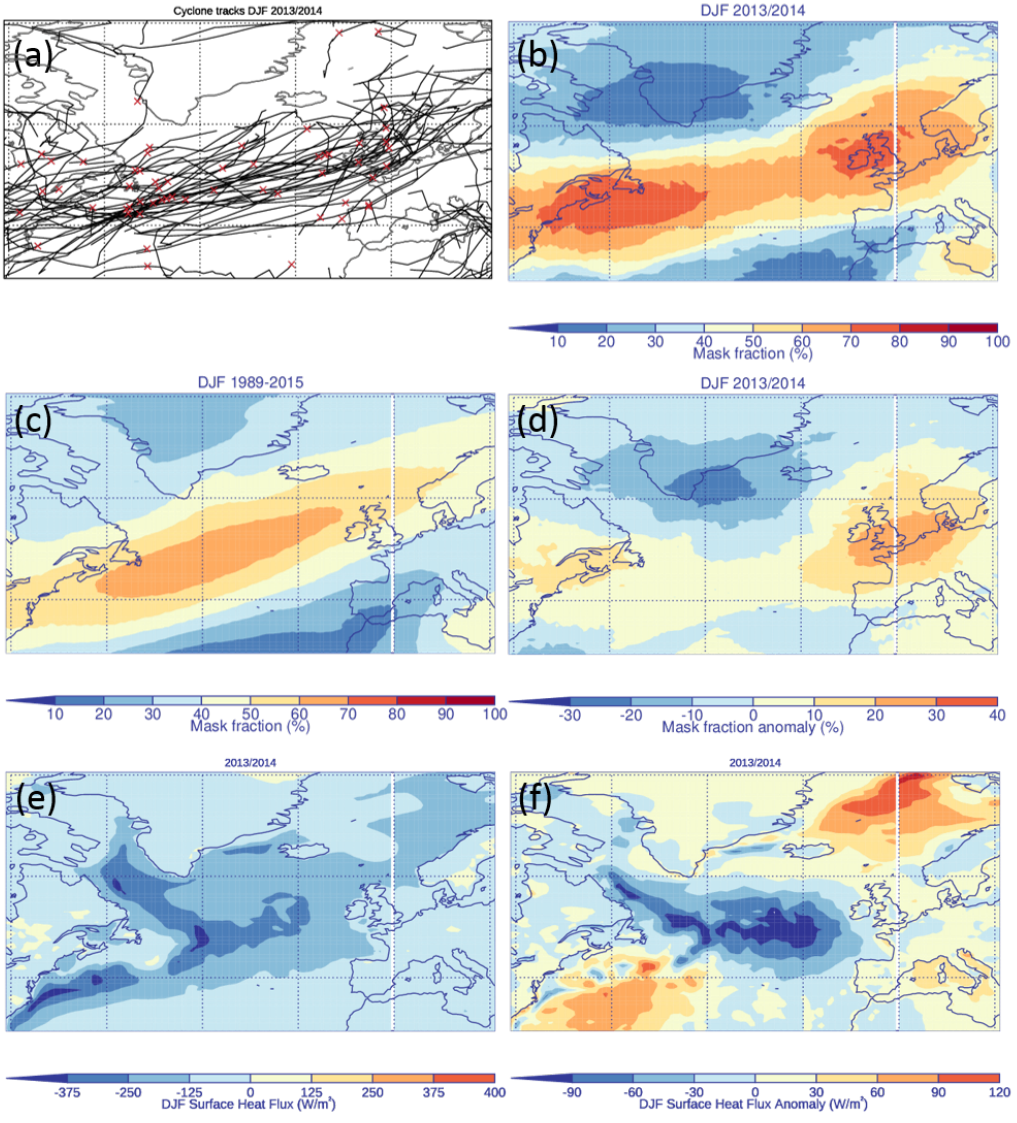

Figure 8. (a) 2013/2014 cyclone tracks (black) with position of maximum intensity (red crosses), (b) 2013/2014 fraction of time within cyclone mask, (c) 1989-2015 mask fraction, (d) anomalous mask fraction, (e) 2013/2014 Q_N (W/m^{-2}) and (f) anomalous Q_N (W/m^2).

https://doi.org/10.5194/wcd-2019-6
Preprint. Discussion started: 13 September 2019

Weather and Climate Dynamics Discussions
Open Access
EGU

4.1 Cyclone associated heat flux

To calculate Q_N due to the cyclones the cyclone tracks for that season are combined with a masking method. A cyclone mask is calculated for each time step where the regions influenced by a cyclone are given a value of one (i.e., they are inside the cyclone mask) and regions that are not influenced are given a value of zero (i.e., they are outside the cyclone mask) (Hawcroft et al., 2012; Sinclair and Dacre, 2019). The heat flux associated with cyclones are asymmetric around the cyclone (figures 6(d)-(f)). Large negative flux is found close to the cyclone centre and extending along the trailing cold front which lies to the west of the cyclone centre. To account for this, a cyclone mask at a given time, t, is created by identifying the position of a cyclone and also it's position during the previous 30 hours. A mask is created which extends $14°$ in a radial circle from each track point, creating an elongated oval shape which encompasses both the cyclone centre and the elongated cold front (figure 9).

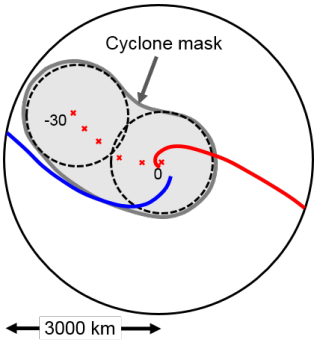

Figure 9. Schematic of cyclone masking method. Red and Blue lines show the approximate position of the cyclone warm and cold front respectively. Red crosses shows the position of a given cyclone at time (t) and at 6-hourly intervals up until 30 hours previously (-30). The outer circle shows the 30 degree radius circle used to produce the composites in figures 4 to 7. The smaller dashed circles show example locations of a 14 degree radius circle centred on the cyclone position at t=0 and t=30. The grey shading shows the extent of the cyclone mask.

Figures 10(a) and (b) show UK Met Office synoptic analysis charts at 00UTC on 24 and 20 December 2013 respectively. At both times there is a low pressure centre situated to the west of Scotland and long trailing cold fronts extending across the north Atlantic. Figures 10(c) and (d) show Q_N at the corresponding times and figures 10(e) and (f) show the cyclone masks. The red lines shows the full track of the cyclones and the elongated oval masks the location of the cyclones at the analysis time and 30 hours earlier. The mask captures Q_N surrounding the cyclone centres and along the trailing cold front. Sensitivity tests have been performed using a radial circle ranging from 10-17° and masks extending 18 to 42 hours prior to the analysis time.

Figure 11(a) shows the contribution to the DJF Q_N anomaly that occurs within a cyclone mask and figure 11(b) shows the contribution that occurs outside a cyclone mask. In the mid-North Atlantic (black box in figure 11(a)) cyclones are responsible for over 78% of the total Q_N anomaly. Since the cyclone mask in this region occurs on average 60% of the time (figure 8(b)), cyclones lead to a higher than average cooling in the mid-Atlantic during the 2013/2014 DJF season. Varying the size of the cyclone mask radius from $10 - 17°$ results in a cyclone contribution from $64 - 84\%$ and a mask fraction from $47 - 71\%$ respectively. Varying the length of the cyclone mask from $18 - 42$ hours results in a cyclone contribution from $72 - 85\%$ and

https://doi.org/10.5194/wcd-2019-6
Preprint. Discussion started: 13 September 2019

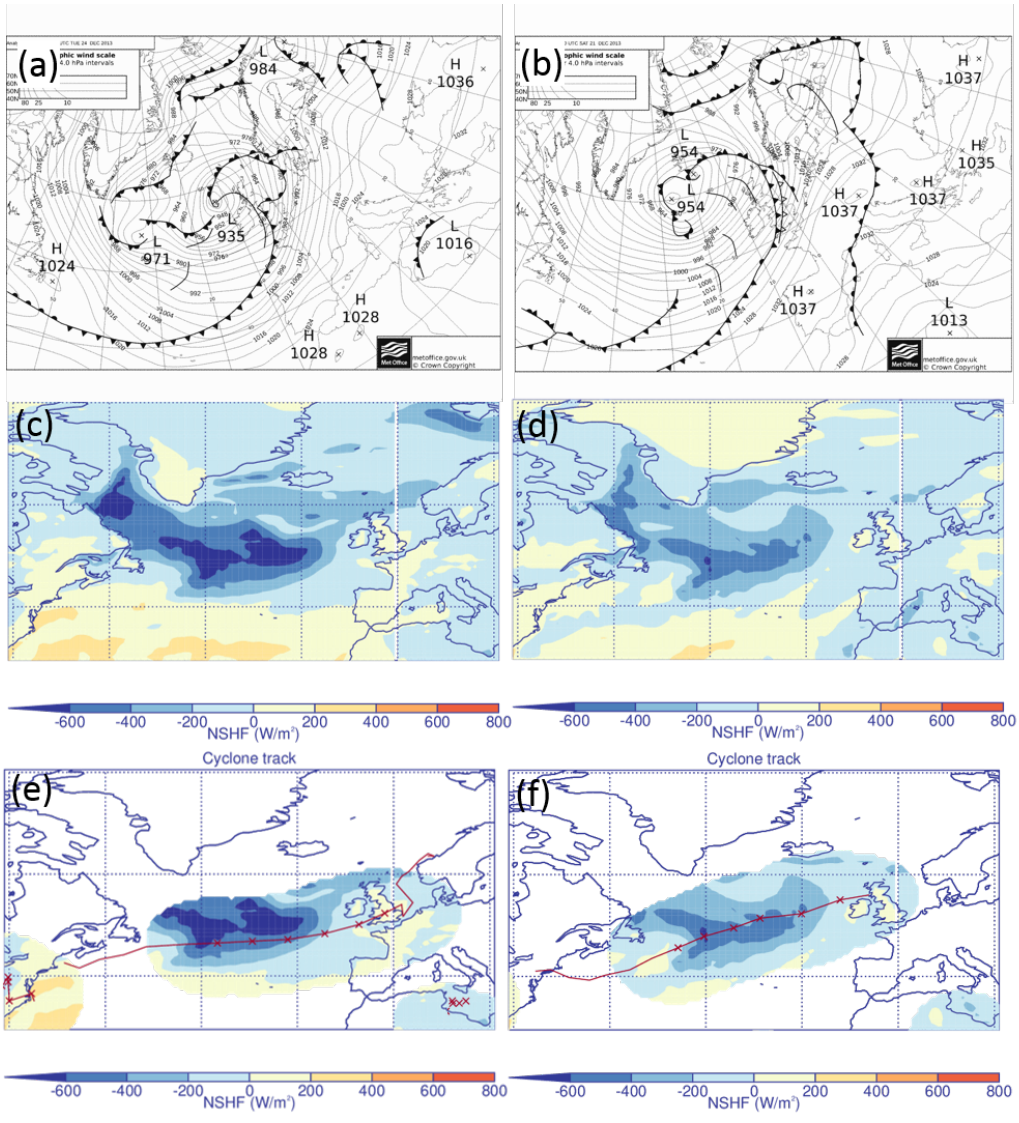

Figure 10. (a,b) UK Met Office synoptic analysis charts, (c,d) Q_N (W/m^2), (e,f) cyclone mask overlaid with tracks for (a,c,e) 00 UTC 24 December 2013 and (b,d,f) 00 UTC 20 December 2013. Red crosses show the position of cyclones at the analysis time and 30 hours previously.

a mask fraction from $55-70\%$. Thus the difference between the cyclone contribution and the mask fraction for all variations ranges from $14-18\%$ suggesting that the conclusion is does not depend on the choices used to define the cyclone mask.

https://doi.org/10.5194/wcd-2019-6
Preprint. Discussion started: 13 September 2019

Weather and Climate Dynamics Discussions
Open Access
EGU

4.2 2013/2014 SST anomalies

In order to determine the contribution of anomalous Q_N in the 2013/2014 season to the seasonal SST anomaly we combine the 2013/2014 Q_N (figure 8(c)) with the monthly DJF 2013/2014 mixed layer depth using equation 1. Figure 11(a) shows the anomalous ΔSST_{Q_N} during the 2013/2014 DJF season. The overall pattern is similar to the Q_N anomaly (figure 8(b)) with enhanced cooling in the mid north Atlantic and reduced cooling to the north and south. Within the region of interest (black boxes in figures 11(c) and (d)) the average SST cooling anomaly due to Q_N is 1 K. Figure 11(d) shows the total SST tendency anomaly from ERA-Interim for the 2013/2014 DJF period. The average SST cooling anomaly in the black box is 1.4 K. Thus net surface heat fluxes in the 2013/14 DJF season account for 70% of the observed anomalous cooling in the mid-North Atlantic. This suggests that entrainment is not particularly important in generating the anomaly, despite the fact that cyclones are typically associated with strong winds.

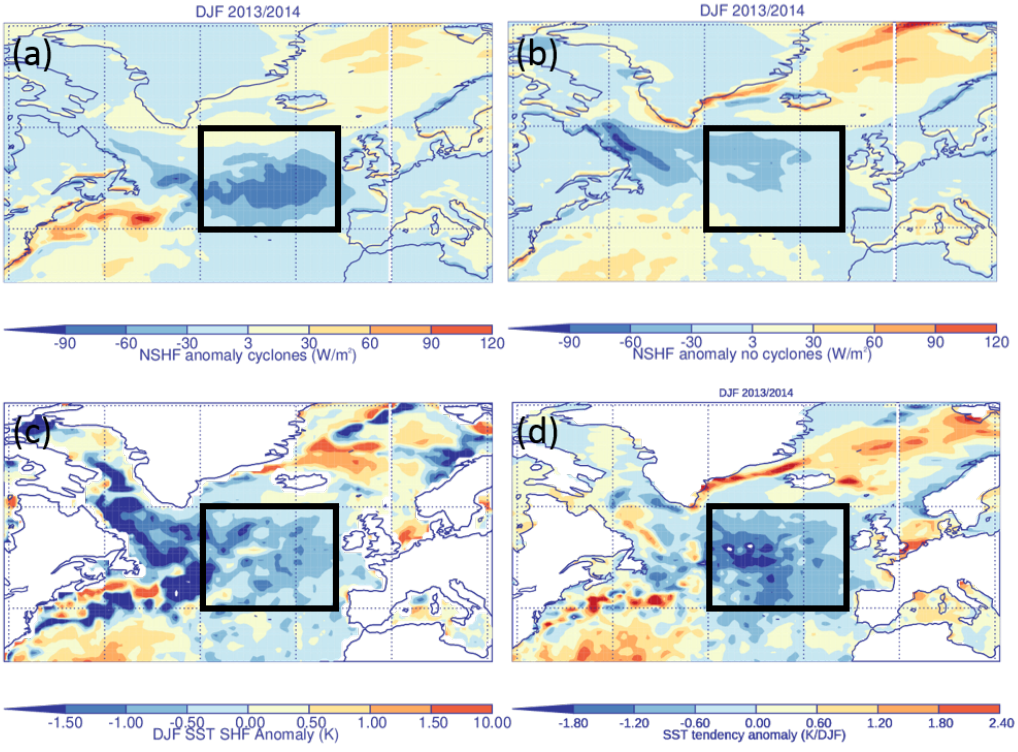

Figure 11. DJF 2013/2014 (a) anomalous Q_N associated with cyclones (W/m^2), (b) anomalous Q_N not associated with cyclones (W/m^{-2}), (c) anomalous ΔSST_{Q_N} (K/DJF) and (d) anomalous ΔSST_{TOT} (K/DJF). The black boxes show the region over which the contribution of ΔSST_{Q_N} to ΔSST_{TOT} is calculated.

https://doi.org/10.5194/wcd-2019-6
Preprint. Discussion started: 13 September 2019

Weather and Climate Dynamics Discussions
Open Access
EGU

5 Conclusions

In this paper we investigate both the SST cooling associated with individual cyclones and the SST cooling associated with the passage of multiple cyclones over the same location in the 2013/2014 season to determine how significant cyclones were in contributing to the observed cooling. We find that enhanced air-sea exchange of heat and moisture in the cold sector behind the cold front of an extratropical cyclone can lead to cooling of up to 0.2 K/day for the strongest cyclones. This cooling is relatively small compared to the variabilty in SST tendency in the North Atlantic, thus the 'cold-wake' associated with the passage of an individual extratropical cyclone is difficult to observe in the instantaneous SST field.

During the 2013/2014 DJF season there were a high number of cyclones and their tracks were anomalously zonal compared to climatology. This resulted in anomalously large negative heat fluxes in a zonal band extending from the east coast of the US towards Europe. Extratropical cyclones were found to be associated with higher than average cooling. Cyclones accounted from $64-85\%$ of the net surface heat flux in the mid-North Atlantic. Furthermore, the net surface heat fluxes in the 2013/2014 season accounted for 70% of the observed cooling in the mid-North Atlantic. Thus, extratropical cyclones have been found to have played a major role in determining the extreme 2013/2014 winter season SST cooling.

Author contributions. H.F.Dacre performed the data analysis for this publication. S.A.Josey and A.L.M.Grant contributed to the scientific interpretation of the analysis.

Competing interests. The authors declare that they have no conflict of interest.

Acknowledgements. The ERA-Interim data were obtained freely from http://apps.ecmwf.int/datasets/. The ORAS5 data were obtained freely from the Integrated Climate Data Center at University of Hamburg http://icdc.cen.uni-hamburg.de. Information on how to obtain the cyclone identification and tracking algorithm can be found from http://www.nerc-essc.ac.uk/ kih/TRACK/Track.html. We thank Kevin Hodges for providing his ETC tracking code.

https://doi.org/10.5194/wcd-2019-6
Preprint. Discussion started: 13 September 2019

Weather and Climate Dynamics Discussions
Open Access
EGU

References

Alexander, M. A. and Scott, J. D.: Surface flux variability over the North Pacific and North Atlantic oceans, Journal of climate, 10, 2963–2978, 1997.

Catto, J. L., Shaffrey, L. C., and Hodges, K. I.: Can climate models capture the structure of extratropical cyclones?, Journal of Climate, 23, 1621–1635, 2010.

Courtois, P., Hu, X., Pennelly, C., Spence, P., and Myers, P. G.: Mixed layer depth calculation in deep convection regions in ocean numerical models, Ocean Modelling, 120, 60–78, 2017.

Crawford, G. and Large, W.: A numerical investigation of resonant inertial response of the ocean to wind forcing, Journal of physical oceanography, 26, 873–891, 1996.

Dacre, H. F., Hawcroft, M. K., Stringer, M. A., and Hodges, K. I.: An extratropical cyclone atlas: A tool for illustrating cyclone structure and evolution characteristics, Bulletin of the American Meteorological Society, 93, 1497–1502, 2012.

Dacre, H. F., Martinez-Alvarado, O., and Mbengue, C. O.: Linking atmospheric rivers and warm conveyor belt airflows, Journal of Hydrometeorology, 2019.

Dee, D. P., Uppala, S., Simmons, A., Berrisford, P., Poli, P., Kobayashi, S., Andrae, U., Balmaseda, M., Balsamo, G., Bauer, d. P., et al.: The ERA-Interim reanalysis: Configuration and performance of the data assimilation system, Quarterly Journal of the royal meteorological society, 137, 553–597, 2011.

Fisher, E. L.: Hurricanes and the sea-surface temperature field, Journal of meteorology, 15, 328–333, 1958.

Grist, J. P., Josey, S. A., Jacobs, Z. L., Marsh, R., Sinha, B., and Van Sebille, E.: Extreme air–sea interaction over the North Atlantic subpolar gyre during the winter of 2013–2014 and its sub-surface legacy, Climate dynamics, 46, 4027–4045, 2016.

Hawcroft, M., Shaffrey, L., Hodges, K., and Dacre, H.: How much Northern Hemisphere precipitation is associated with extratropical cyclones?, Geophysical Research Letters, 39, 2012.

Hodges, K.: Feature tracking on the unit sphere, Monthly Weather Review, 123, 3458–3465, 1995.

Kawai, Y. and Wada, A.: Detection of cyclone-induced rapid increases in chlorophyll-a with sea surface cooling in the northwestern Pacific Ocean from a MODIS/SeaWiFS merged satellite chlorophyll product, International journal of remote sensing, 32, 9455–9471, 2011.

Kleinschmidt, E.: Principles of the theory of tropical cyclones, Arch. Meteor. Geophys. Bioklimatol, 4, 53–72, 1951.

Kobashi, F., Doi, H., and Iwasaka, N.: Sea surface cooling induced by extratropical cyclones in the subtropical North Pacific: Mechanism and interannual variability, Journal of Geophysical Research: Oceans, 124, 2179–2195, 2019.

Nelson, J., He, R., Warner, J. C., and Bane, J.: Air–sea interactions during strong winter extratropical storms, Ocean Dynamics, 64, 1233–1246, 2014.

Ogawa, F. and Spengler, T.: Prevailing Surface Wind Direction during Air-Sea Heat Exchange, Journal of Climate, 2019.

Papritz, L., Pfahl, S., Sodemann, H., and Wernli, H.: A climatology of cold air outbreaks and their impact on air–sea heat fluxes in the high-latitude South Pacific, Journal of Climate, 28, 342–364, 2015.

Parfitt, R., Czaja, A., and Kwon, Y.-O.: The impact of SST resolution change in the ERA-Interim reanalysis on wintertime Gulf Stream frontal air-sea interaction, Geophysical Research Letters, 44, 3246–3254, 2017.

Persson, G., Ola, P., Hare, J., Fairall, C., and Otto, W.: Air–sea interaction processes in warm and cold sectors of extratropical cyclonic storms observed during FASTEX, Quarterly Journal of the Royal Meteorological Society: A journal of the atmospheric sciences, applied meteorology and physical oceanography, 131, 877–912, 2005.

https://doi.org/10.5194/wcd-2019-6
Preprint. Discussion started: 13 September 2019

Pettersen, S., Bradbury, D. L., and Pedersen, K.: The Norwegian cyclone models in relation to heat and cold sources, Geophysica Norvegica, 1962.

Priestley, M. D., Pinto, J. G., Dacre, H. F., and Shaffrey, L. C.: The role of cyclone clustering during the stormy winter of 2013/2014, Weather, 72, 187–192, 2017.

Ren, X., Perrie, W., Long, Z., and Gyakum, J.: Atmosphere–ocean coupled dynamics of cyclones in the midlatitudes, Monthly weather review, 132, 2432–2451, 2004.

Rudeva, I. and Gulev, S. K.: Composite analysis of North Atlantic extratropical cyclones in NCEP–NCAR reanalysis data, Monthly Weather Review, 139, 1419–1446, 2011.

Schemm, S. and Sprenger, M.: Frontal-wave cyclogenesis in the North Atlantic–a climatological characterisation, Quarterly Journal of the Royal Meteorological Society, 141, 2989–3005, 2015.

Shaman, J., Samelson, R., and Skyllingstad, E.: Air–sea fluxes over the Gulf Stream region: Atmospheric controls and trends, Journal of Climate, 23, 2651–2670, 2010.

Sinclair, V. and Dacre, H.: Which Extratropical Cyclones Contribute Most to the Transport of Moisture in the Southern Hemisphere?, Journal of Geophysical Research: Atmospheres, 124, 2525–2545, 2019.

Tanimoto, Y., Nakamura, H., Kagimoto, T., and Yamane, S.: An active role of extratropical sea surface temperature anomalies in determining anomalous turbulent heat flux, Journal of Geophysical Research: Oceans, 108, 2003.

Toyoda, T., Fujii, Y., Kuragano, T., Kamachi, M., Ishikawa, Y., Masuda, S., Sato, K., Awaji, T., Hernandez, F., Ferry, N., et al.: Intercomparison and validation of the mixed layer depth fields of global ocean syntheses, Climate Dynamics, 49, 753–773, 2017.

Vannière, B., Czaja, A., Dacre, H., and Woollings, T.: A "cold path" for the Gulf Stream–troposphere connection, Journal of Climate, 30, 1363–1379, 2017.

Yao, Y., Perrie, W., Zhang, W., and Jiang, J.: Characteristics of atmosphere-ocean interactions along North Atlantic extratropical storm tracks, Journal of Geophysical Research: Atmospheres, 113, 2008.

Zolina, O. and Gulev, S. K.: Synoptic variability of ocean–atmosphere turbulent fluxes associated with atmospheric cyclones, Journal of climate, 16, 2717–2734, 2003.

Zuo, H., Balmaseda, M., de Boisseson, E., Hirahara, S., Chrust, M., and De Rosnay, P.: A generic ensemble generation scheme for data assimilation and ocean analysis, European Centre for Medium-Range Weather Forecasts, 2017.

Zuo, H., Balmaseda, M. A., Tietsche, S., Mogensen, K., and Mayer, M.: The ECMWF operational ensemble reanalysis–analysis system for ocean and sea ice: a description of the system and assessment, Ocean Science, 15, 779–808, 2019.